Inexorable land degradation due to agriculture expansion in South American Pampa

Anthony Foucher[1], Marcos Tassano[2], Pierre-Alexis Chaboche[1], Guillermo Chalar[3] Mirel Cabrera[2], Joan Gonzalez[2], Pablo Cabral[2], Anne-Catherine Simon[4], Mathieu Agelou[4], Rafael Ramon[5], Tales Tiecher[6], Olivier Evrard[1]

1. Laboratoire des Sciences du Climat et de l'Environnement (LSCE-IPSL), UMR 8212 (CEA/CNRS/UVSQ), Université Paris-Saclay, 91191 Gif-sur-Yvette Cedex, France
2. Laboratorio de Radioquímica, Área de Radiofarmacia, Centro de Investigaciones Nucleares, Facultad de Ciencias, Universidad de la República, PC:11400, Mataojo 2055, Uruguay
3. Sección Limnología, Facultad de Ciencias, Instituto de Ecología y Ciencias Ambientales, Facultad de Ciencias, Universidad de la República, Uruguay
4. Université Paris-Saclay, CEA, List, F-91120 Palaiseau, France
5. BASF SA, Environmental Fate - Regulatory Science Crop Protection, Avenida Brasil, 791, Guaratinguetá, São Paulo, Brazil
6. Department of Soil Science, Federal University of Rio Grande do Sul (UFRGS), Bento Gonçalves Ave. 7712, 91540-000 Porto Alegre, RS, Brazil

Corresponding author: Anthony Foucher (anthony.foucher@lsce.ipsl.fr)

Abstract

From 1985 onwards, South America has undergone a major expansion of agriculture at the expense of native vegetation (e.g. native Pampa grassland). As an emblematic crop, the surface area cultivated with soybeans has increased by 1000% between 1990 and 2020 in Uruguay. The environmental consequences of this massive land use conversion on soil degradation remain poorly documented although the agriculture expansion is projected to continue to increase in the coming years in South America. In this study, sediment cores were collected in reservoirs located downstream of two contrasted agricultural catchments draining the Rio Negro River (Uruguay) for reconstructing the sediment dynamics and the sources of erosion associated with this expansion.

Results demonstrated the occurrence of two periods of acceleration of sediment delivery since the 1980s. The first period of acceleration was recorded in the mid-1990s and was related to afforestation programs. The second and larger acceleration phase was recorded after 2000 during the soybean crop expansion. This period has been marked by a greater supply of sediment from the native grassland source highlighting the impact of agriculture expansion at the expense of native vegetation. Conservation measures should therefore be urgently taken to preserve biodiversity and soil functions in this region.

Introduction

Agricultural production has significantly increased in countries of the Northern Hemisphere (e.g. those in Europe and North-America) from the 1950s onwards to respond to the global food demand [1]. This increase mainly relied on the modernization of agricultural practices (e.g. mechanization, fertilizers, genetic modifications of plants) and the implementation of major landscape changes. In other regions of the world like in South-America, a second phase of agricultural intensification occurred after 1985 with the expansion of the cultivated land area and extensive livestock breeding in zones that were previously not cultivated [2]. This modern cultivation mode has been associated with a greater use of chemicals inputs, the sowing of genetically modified species (e.g. with genotypes resistant to glyphosate) and changes in agricultural practices with the implementation of monoculture and no-till farming. Since the mid-1980s, surfaces occupied by pasture, cropland and commercial plantations increased by 23, 160, 288% respectively in South-America [3]. Among these widespread land use changes, the surface devoted to soybean cultivation doubled (from 26.4 Mha to 55.1 Mha) between 2000 and 2019 on grassland that had been previously converted from natural vegetation for cattle production [4]. By 2018, 40% (713Mha) of the South-American land mass was significantly impacted by human activities [3]. Uruguay is one of the emblematic countries associated with this agricultural expansion at the expense of natural ecosystems. The generalization of soybean cultivation after 2000 was accompanied by a process of "intensification" of land use, with annual double cropping in both winter and summer, a process that is observed nowadays across more than 30% of the country area [5]. Although agricultural growth occurred mainly in the traditional agricultural areas, it has also affected areas without previous agricultural activity that used to be covered with natural vegetation. This agricultural expansion is mainly explained by the arrival of new farmers and internal/external investors.

Land degradation refers to the processes such as soil erosion that drive the deterioration of all terrestrial ecosystems (IPBES glossary). A recent study (2008) demonstrated that 80% of Uruguayan soils [6] are affected by soil degradation (, i.e. the diminishing capacity of the soil to provide ecosystem goods and services as desired by its stakeholders, according to the IPBES glossary). To combat erosion, a soil conservation policy was implemented from 2014 onwards in Uruguay. It required the presentation of Responsible Soil Use and Management Plans [7], the adoption of no-tillage while leaving the soil covered with vegetation and the implementation of rotations with pastures in order to mitigate water erosion across the country. The adoption of this policy succeeded in reducing erosion per unit area, although gross erosion continued to increase as a result of agricultural expansion through the replacement of natural grassland with cropland in other regions of Uruguay [8]. To the best of our knowledge, no regional study quantified changes in soil erosion in this part of the world, although a few studies conducted at the scale of small catchments documented the impact of land use changes and the adoption of no-tillage on soil erosion [9]. In Southern Brazil, in catchments managed with no-till practices, very high sediment fluxes were recorded for the 2011-2015 period (37–259 t km^{-2} yr^{-1}), which demonstrates that the sustainability of the soil cultivation system is threatened [10]. Beyond the *on-site* consequences of soil erosion (e.g. loss of fertility and decrease in crop yields), multiple *off-site* effects threaten water quality with the excessive transfer of potentially contaminated sediment to the hydrosystems [11]. In Uruguayan (<20 km²) and Brazilian catchments (respectively <20 and 804 km²), cropland was identified to supply the main source of sediment (>70% of the contribution) [12,13]. This excessive supply of sediment from upper catchment parts contributes to the degradation of water quality and to the siltation of water bodies. Accordingly, a significant reduction in the storage capacity of reservoirs used to supply drinking and irrigation water, as well as for hydroelectric power production (respectively 63.5% and 60% of Brazilian and Uruguayan energy production) is expected. Beyond the degradation of land and water resources, this second phase of agricultural expansion after 1985 induced a massive loss of biodiversity with the destruction of natural habitats (primary forests, natural grasslands, freshwater) [14], and raised several concerns regarding human health [15] and ecosystem services [16].

Although the environmental consequences of the “agricultural revolution” that took place after World War II in Europe and North-America including land degradation were extensively investigated based on modeling, monitoring and paleoenvironmental reconstructions, much less attention has been devoted to the recent and massive expansion of agriculture and its intensification across South-America in general, and in the Campos ecosystem in particular (southern Brazil, northeastern Argentina and Uruguay). To the best of our knowledge, the impact of land cultivation on hydro-sedimentary transfers was investigated in this Campos ecosystem through the use of river gauging stations, plots survey, sediment source fingerprinting and modeling [17] [18] and modeling. These approaches allow to quantify at a high spatial resolution and over relatively short –time scale (<5 years) the impacts of modern farming practices on water and sediment exports. However, they do not allow to monitor or reconstruct the inertia, magnitude and resilience of continental ecosystems that occurred over longer time scales (>10 years), i.e. including the conversion of Campos into cultivated land and commercial plantations.

Collecting and analyzing sediment accumulated in reservoirs provide a powerful tool to achieve these reconstructions [19]. Paleoenvironmental reconstructions were successfully applied at different timescales (e.g. Holocene [20]) and in various agricultural contexts for reconstructing the adverse consequences of agriculture on sediment delivery [21], transfer of contaminants [22] or eutrophication [23].

To the best of our knowledge, few paleoenvironmental studies focused on the processes that occurred during the last decades in South-America in general, and in the Campos ecosystems area in particular. One of the reasons for the lack of paleoenvironmental studies in this region highly impacted by anthropogenic pressures is the small number of lakes and reservoirs draining these agricultural areas.

In the current research, we have retrospectively investigated the consequences of land use conversion on land degradation by analysing sediment cores (PA-02 and RDB-01 cores) collected in two large reservoirs (the Palmar (PA) and Rincón del Bonete (RDB reservoirs) draining the Rio Negro river in Uruguay (Fig. 1, Fig.2). A limnogeological approach based on dating (using artificial and natural radionuclides including caesium-137 (^{137}Cs) and excess of lead-210 ($^{210}Pb_{ex}$)) and characterizing the sedimentary sequences with multiple analyses (e.g. organic matter properties (Total Organic Carbon (TOC), Total Nitrogen (TN) and stable isotope measurements ($\delta^{13}C$ and $\delta^{15}N$), X-ray fluorescence core scanner (XRF), tomography scanner (CT-Scan)) was conducted in order to (1) reconstruct the changes in sediment delivery based on the mass accumulation rates (MAR) and terrigenous XRF proxy (Fe and Ti) associated with the last and massive expansion of agriculture in Uruguay (1982-2019), (2) identify the main sources of land degradation accumulated in the reservoirs and quantify the respective contributions of cropland (CR) and natural grassland (NG) sources to sediment and, finally, (3) outline the main drivers of land and water degradation. Accordingly, the general goal of this study is to better understand the history and drivers of the sediment cascade in this region in order to reduce the deleterious consequences of modern agriculture at a time when this intensification is projected to continue in the coming decades.

Results

Core description and chronology

The RDB-01 and PA-02 sequences were composed of homogenous fine brown-coloured sediment. No specific facies or layers were visually observed in these cores. CT-Scan images allowed to detect some coarser/denser particle levels at the bottom of the PA-02 core only, whereas such levels were not observed on the RDB-01 core.

The $^{210}Pb_{ex}$ activity along the RDB-01 core decreased according to a linear trend (r^2= 0.89) (Fig. 3a). The application of the CF:CS (Constant Flux: Constant Sedimentation) model allowed to date the base of this 31 cm long sequence to 1992 (± 3 years) with an average sedimentation rate (SAR) of 11 mm yr^{-1}. The first appearance of ^{137}Cs was detected between 27 and 31 cm depth in the RDB-01 core (3 Bq kg^{-1}, SD 0.4 Bq kg^{-1}), and a very low ^{137}Cs peak was observed between 12 and 15 cm depth (4.2 Bq kg^{-1}, SD 0.7 Bq kg^{-1}). The characteristic peak typically associated with the maximum ^{137}Cs bomb fallout (1964-1965 in South-America [24]) was logically not observed in this recent sediment sequence (Fig. 3a) in agreement with previous plutonium isotope measurements performed on this core, which demonstrated that sediment deposited well after this period [25].

The $^{210}Pb_{ex}$ activity from the PA-02 core decreased according to a linear trend as well (r^2= 0.94. The age-depth model based on the CF:CS model allowed to date the base of the sequence to 1978 (± 4 years) with an average SAR of 5.5 mm yr^{-1} (Fig. 3b). In the PA-02 core, ^{137}Cs was detected along the entire sedimentary sequence with a maximal value recorded between 9 and 12 cm depth (5.1 Bq kg^{-1}, SD 0.8 Bq kg^{-1}, corresponding to the period between 1997 and 2002 according to the $^{210}Pb_{ex}$ dating). As for the RDB-01 core, no peak that may have been attributed to the thermonuclear bomb testing was observed in this post-1965 sequence. The PA-02 age-model was validated by both field and CT-scan observations. During sampling, a paleo-soil was observed at the base of the core and the occurrence of denser particles was detected with CT-Scan images. These observations were in agreement with the CF:CS model outputs dating the base of the core to 1978 (± 4 years), corresponding approximatively to the age of the dam commissioning (1982).

Organic matter properties

In both reservoirs, the organic fraction represented only a low proportion of the total material inputs (including both autochthonous and allochthonous inputs). In the RDB-01 sequence, the average TOC content reached 3.0 ±0.2% of the dry sediment with a maximal value recorded in 2001 (3.7%) (Fig. S1). In the PA-02 sediment core, the average TOC content amounted to 3.5 ±0.2% with minimal values recorded between 2000-2011 and a maximal value in 1985 (respectively, 3.2 and 3.75%) (Fig. S2).

The RDB sequence demonstrated the occurrence of two periods of changes in organic matter sources between 1992 and 2019 (Fig. S1). These periods were associated with simultaneous changes in TN, C:N ratio and $\delta^{13}C$. They took place between 1996-2002 and between 2013-2019. During these periods, TN increased by an average value of 0.31% (±0.03%), whereas C:N ratio and $\delta^{13}C$ decreased (respective average values of 10 ±0.7% and -20.1 ±0.55‰). Nitrogen isotope variations highlighted the occurrence of distinct periods before and after 2001. Before this period, $\delta^{15}N$ amounted on average to 6.2 ±0.7 ‰), whereas after this period it reached around 8 ±0.5‰ (Fig. S1).

Both TN and $\delta^{13}C$ proxies showed significant changes along the PA-02 sequences (Fig. S2). TN increased in 1984, in 1996 (0.29% rise for both change periods) and even more significantly between 2015 and 2019 (0.31% rise). The $\delta^{13}C$ showed an increase during the 1993-2000 period and in 2019. The largest change was observed in 2012 (from -20.1‰ in 2009 to -21.4‰ in 2019). In contrast, no sudden change nor peak in C:N ratio was observed along the sequence. Nevertheless, a constant decrease of the C:N ratio was detected from the base (13.1) to the top (10.7) of the sequence (Fig. S2).

Terrigenous proxies and MAR evolution

Both proxies of the terrigenous fraction (Ti and Fe) were highly correlated in both the RDB-01 and PA-02 cores (with respective r^2 values of 0.96 and 0.87). A significant positive trend of terrigenous inputs was recorded in these sequences (MK-test p-value >0.01). In the RDB core, three periods of dominant terrigenous delivery were recorded between 1992 and 1998, between 2004 and 2008 and between 2012-2019 (Fig. S1). In contrast, the 1998-2004 period recorded a decrease of this terrigenous contribution. In the PA-02 sequence, similar periods of increase were observed between 1992 and 1996, between 2004 and 2011 as well as between 2013 and 2019 (Fig. S2), whereas no period of decrease was observed in the PA-02 core.

Like the terrigenous Ti and Fe proxies, the MAR calculated for both reservoirs showed a significant positive trend (MK-test p-value >0.01) in sediment delivery (Fig. 4). In the RDB sediment core, three main periods of greater accumulation of sediment were observed, in 1992-1998, 2004-2008 and 2012-2019 (with corresponding average MAR values of 0.16, 0.17 and 0.18 g cm^{-2} $year^{-1}$) as well as one period of decrease between 1999 and 2002 (with a minimum in 2001, and a MAR of 0.11 g cm^{-2} $year^{-1}$) (Fig.4). In the Palmar reservoir, three main periods of high mass accumulation of sediment were also recorded between 1991 and 1995, 2006 and 2011 and between

2013 and 2019 (with average MAR values for these periods of 0.15, 0.16 and 0.18 g cm^{-2} $year^{-1}$). A major period of decrease of sediment inputs was also observed in 2002 (with a MAR of 0.14 g cm^{-2} $year^{-1}$) (Fig. 4).

Sediment sources

Among the potential organic matter properties used for tracing the sources of sediment, TN allowed to reclassify 76% of the source samples whether they originated from natural grassland or cropland sources. The sediment fingerprinting results indicate that in both reservoirs, the dominant sources of sediment were associated with the cropland sources (in average 75.0 ±5.0% and 74.5 ±1.5%) for the RDB-01 and PA-02 sequences) (Fig. 4). In the PA sequences, the lowest contribution of natural grassland source was recorded around 1993 (22%) while the highest was found around 1984 and 1997 (28%). No significant trend of change in source contributions was observed in this reservoir. In the RDB-01 core, the lowest contribution of natural grassland was observed in 2012 (18%) whereas the maximal contribution of this source was detected in 2018 (39%). In addition, four peaks of the natural grassland source contribution were detected in 1994, 2001, 2013, 2015 (supplying respectively 29, 33, 31 and 32% of sediment). The natural grassland contribution has increased on average by 58% between 2002 and 2018 (Fig. 4) in the RDB sequence. Nevertheless, this trend was found not to be significant (MK-test p-value <0.01).

Discussion

During its recent history (<70 years), the Palmar catchment was impacted as the southern and western parts of Uruguay by a first expansion phase of agriculture during the 1950s, whereas both Palmar and Rincón del Bonete catchments experienced another period of intensification and expansion of agriculture after the 1980s [26]. In response to this land conversion, the reservoirs recorded a sediment delivery increase of 33 and 7% on average since 1982 and 1992 and until 2019 in the PA-02 and the RDB-01 cores (Fig. 4). This period was associated with a dominant contribution of the cropland source (>70%) as previously reported in other studies conducted in Uruguay and Southern Brazil [12,13] and characterised by a strong correlation between the sediment dynamics (MAR) and the cultivated surface area available from the FAO database (e.g. r^2 of 0.84 for the 1982-2019 period in the PA reservoir).

In details, a first acceleration was identified in the PA reservoir between 1990 and 1995 (peaking in 1993) and was characterized by an increase of the MAR, the Fe proxy and by a decrease in $\delta^{13}C$ values. In the RDB sequence, the 1990s displayed the same trend (increase of the MAR and of the Fe proxy) with an increase of sediment accumulation during the 1992-1998 period. In Uruguay, planting of non-indigenous trees and installation of farms for agroforestry has been common for a long time (e.g. for providing windbreaks and shelters for livestock, poles, firewood production) [27]. However, the 1990s paved the way to industrial planting with the entry into force of the forestry law encouraging investors to convert land into profitable forests, while major constraints were introduced for farming (cultivation) and livestock grazing areas, which impacted in turn the productive capacity. The higher internal and external demands in wood products also facilitated the expansion of afforestation zones in "better quality" soil areas [28]. In the RDB catchment, approximately 6,000 km² of non-indigenous trees were planted between 1990 and 2001 with an increase of the planted area from 500 km² in 1988 to 6,610 km² in 2001 [29]. A similar situation was observed in the PA basin, although to a lesser extent. As a response to the eucalyptus and pine planting, the mass accumulation rates of sediment increased by 27% and 21% in the RDB and PA reservoirs. To the best of our knowledge, only few records of erosion rates are available at the plot or at the catchment scale in areas affected by eucalyptus afforestation in Uruguay [9]. Nevertheless, in the neighboring State of Rio Grande do Sul in southern Brazil, soil erosion rates were measured in such plots and values ranging between 3 and 6379 t km^{-2} $year^{-1}$ were found depending on the soil properties and the number of years since the plantation [30]. As reported by the authors, after the plantation, erosion rates decreased rapidly as the canopy covered the soil surface by reducing the soil exposure to raindrops and runoff. Erosion was measured to decrease from 620 to 110 t km^{-2} $year^{-1}$ from 2 to 7 years after the plantation [30] under the effect of the tree growth and the progressive cover of the soils with vegetation. The sediment delivery trajectories recorded for the RDB and PA cores are in agreement with these findings, which may explain the decrease of sediment inputs into the reservoirs several years after the implementation of afforestation programs, after an initial phase of increase (Fig. 4). This afforestation period was associated with a greater contribution of the natural grassland source to the RDB core (contribution of 29% in 1994) whereas only a slight increase of cropland source was observed in the PA sequence (contribution of 78% in 1993). These different sediment source signatures suggest the occurrence of two strategies of land conversion in relation with the catchment history. In the PA catchment, the historically cultivated land (e.g. mostly mixed-farming with the alternation of crops and livestock) was converted into artificial forests (e.g. mainly on the soils with the largest constraints to produce annual crops). In contrast, in the RDB catchment, the natural grassland (e.g. used for livestock farming) was converted for afforestation purposes. Despite some studies suggest a decrease of soil erosion after the conversion of degraded grassland into artificial forests [31], the current research recorded a significant acceleration of erosion in both historically and recently farmed catchments.

The highest acceleration was observed between 2002 and 2019 with an increase of sediment delivery by 20 and 67% and that of terrigenous inputs by 19 and 77%, respectively, for the PA and RDB reservoirs. This acceleration occurred during the last phase of agricultural expansion observed just after the economic crisis in Uruguay (2000-2002), which is reflected in the sediment cores by a sharp drop of the accumulation rates in response to the reduction of the cultivated areas (Fig. 4) After 2002, land conversion in Uruguay was strongly impacted by internal (favorable financial climate, decrease of exportation taxes in Uruguay) and external policies (2002 financial collapse and increase of taxes in Argentina), which have resulted in a sudden expansion of soybean cultivation and afforestation of exotic trees [34]. In the RDB catchment, this crop was implemented at the expense of native vegetation and it occupied more than 700 km² in 2019 [29]. This expansion had led to a 58% increase of the natural grassland source contribution to the Bonete sediment sequence. Although grassland is less sensitive to erosion than cultivated soils, the increase of NG contribution to sediment may be explained by the mobilization of particles from ploughed grassland that had been recently converted into cropland and that maintained temporarily their NG signature despite their cultivation during the first years that followed this land use conversion [36]. The greater contribution of the NG and the acceleration of MAR was associated with major changes in organic matter properties in the RDB sequence, which is demonstrated by low values of C:N, $\delta^{13}C$ and a strong increase of TN (Fig. S1). These changes in organic matter properties support the sediment tracing results showing the impact of the extension of the soybean cultivation on the sediment supply observed in the RDB sequence. During the 2002-2019 period, the acceleration of sediment dynamics was strongly correlated to the soybean surfaces cultivated at the country scale (r^2 of 0.67 – unfortunately, no data is available at the catchment scale) (FAO Database) supporting the finding that the soybean expansion was the main driver of land degradation. Other modes of cultivation can also explain this acceleration of sediment inputs such as the increase in the artificial forest surfaces. A more detailed sediment fingerprinting approach that may rely on novel environmental DNA metabarcoding [36] and the analysis of historical data on land use changes may contribute to further improve the unambiguous identification of the main drivers of erosion in this catchment. The PA catchment is located in one of the most productive soybean areas in Uruguay (concentrating more than 50% of the national soybean production). The soybean expansion mainly occurred in former cultivated plots without a massive expansion of agriculture at the expense of native vegetation. Consequently, this likely explains why no significant change in the natural grassland source contribution to sediment was observed in the PA sequence (Fig. 4), contrary to the results found in the RDB sequence, with the increase of sediment supply from NG material recently converted into cropland. Nevertheless, sediment accumulated in the PA reservoir demonstrated as in the RDB core a major increase of sediment accumulation rates associated with the combination of a decrease of the C:N ratio, low values of $\delta^{13}C$ and high values of TN corresponding to a greater contribution of areas cultivated with soybean to sediment (Fig. S2). This expansion of soybean in former cultivated plots induce a less important increase of sediment dynamics in PA sequence that one observed in the RDB core associated to the grassland conversion between 2002 and 2019 (r^2 of 0.91 between the soybean surfaces at the scale of Uruguay and the MAR of the PA core) (FAO database).

As the soybean production is projected to further increase by 50% by 2050 in South-America [37], the results obtained in the current study lead us to anticipate a further acceleration of land and water degradation in this part of the world. This question is crucial for a country like Uruguay, which is socio-economically very much dependent on the quality of soil resources. Beyond the problems directly associated with soil degradation, this agricultural expansion induced a large number of multiple deleterious consequences on terrestrial and aquatic ecosystems, which remain poorly understood. Consumption of NPK fertilizers should be promote in the coming years to compensate the decrease of soil fertility. The import of fertilizers has already tripled between 2000 and 2015 [38]. Some of these nutrients can locally increase the soil acidity in association with a strong carbon print [39] and may reach the hydrographic system where they may further increase eutrophication problems and the frequency and intensity of cyanobacterial blooms. This type of phenomenon is already observed in Uruguay and its occurrence is expected to increase in the coming years, thereby threatening the sustainability and the quality of water resources [40,41]. In addition, a particular attention should be focused on the fate of pesticides massively applied in this area [42] and more specifically on the interaction between the greater use of herbicides (import of herbicides increased by 30% for the 2000-2015 period [38]) and soil erosion, although this relationship needs to be further investigated [21]. The environmental impacts of the massively applied *Mirex* insecticides in eucalyptus plantations should also be looked into. Understanding the adverse consequences of the agriculture expansion in South-America is of paramount importance in order to design and implement mitigation strategies to protect water and soil resources. Furthermore, additional research will be needed to identify in more details the sources of sediment and to characterise the persistence and the potential remobilization of pesticides which could lead to a further degradation of soil and water quality.

Materials and Methods

Sampling

Sediment cores were collected in the Rincon del Bonete (RDB-01, 31 cm long, IGSN number: IEFOU0007) and Palmar (PA-02, 22.5 cm long, IGSN number: IEFOU0006) reservoirs using a 60 mm Uwitec gravity corer equipped with a 0.6 meter PVC liner tube available at the Universidad de la República (Montevideo, Uruguay). Coring sites were selected in the vicinity of the dams in order to avoid sampling of coarser deposits classically found in deltaic areas associated with coarse-grained material deposited during extreme events. Other goals of this strategy were to ensure the collection of sediment at places where the accumulation of fine material is maximal, and to provide good representativeness of all the river inputs transported from the drainage areas into the reservoirs (Fig. 1).

Sediment core dating

Core chronology was established based on the measurements of short-lived fallout radionuclides (caesium-137 (^{137}Cs) and excess of lead-210 ($^{210}Pb_{ex}$)) conducted on 17 samples (respectively 10 samples for the RDB-01 core and 7 samples for the PA-02 core) of dry sediment (≈10g) collected along the sedimentary sequences.

Gamma spectrometry measurements were obtained using coaxial N- and P- type HPGe detectors (Canberra/Ortec) available at the Laboratoire des Sciences du Climat et de l'Environnement (Gif-sur-Yvette, France). Radionuclide data was decay-corrected to June 2020. Sediment ages were determined using the CF:CS model (Constant Flux: Constant Sedimentation), which assumes a constant rate of $^{210}Pb_{ex}$ from atmospheric fallout with a constant rate of sedimentation [43]. These models were automatically computed using the R package SERAC [44]. Age model validation was conducted through the identification of the ^{137}Cs time marker originating from the thermonuclear weapon testing (maximal emissions in 1962) assumed to peak in 1964-65 in sediment archives of South America [24] and through the identification of the underlying paleosoil in the PA sediment core attributed to correspond to the dam commissioning in 1982 for PA. Radionuclide measurements used for the establishment of the core chronology are provided in an open access Zenodo dataset (https://zenodo.org/record/6630369#.YqiGkOzP2Uk).

Non-destructive laboratory analyses

The Avaatech X-ray fluorescence core scanner (XRF) available at the Laboratoire des Sciences du Climat et de l'Environnement was used to obtain high resolution (0.5 cm) and semi-quantitative (cps) values of geochemical element contents along the core. This data was used for characterizing potential changes in sediment sources throughout time. Titanium (Ti) and iron (Fe) proxies were specifically used for identifying changes in detritical material contributions [45].

Non-calibrated sediment density was recorded every 0.6 mm along the sediment sequences using Computer Tomography scanner (CT-Scan) images obtained using the equipment (GE Discovery CT750 HD) available at the DOSEO platform (French Atomic Energy and Alternative Energy Commission, CEA Paris-Saclay, France). Relative density values (derived from CT-number) were extracted from the reconstructed scanner images using the free software ImageJ. The relative values of dry bulk density (DBD) were calibrated by measuring the absolute DBD (g cm^{-3}) in 20 samples collected along the cores (obtaining a r^2 of 0.8 and 0.85 between DBD and CT-number for PA-02 and RDB-01 cores, respectively).

The Mass Accumulation Rate (MAR, expressed in g cm^{-2} yr^{-1}) was reconstructed for each individual core by multiplying the high resolution DBD extracted from the calibrated tomography scanner profiles (expressed in g cm^{-3}) with the Sediment Accumulation Rate (SAR, cm yr^{-1}) provided by the age model following the procedure described by Foucher et al. [19].The MAR corresponds to the amount of organic and terrigenous material deposited at each individual coring site and its evolution throughout the time.

Destructive laboratory analyses

Isotope-Ratio Mass Spectrometry (IRMS) analyses were conducted on dry sediment for determining organic matter properties, including elemental concentrations (Total Organic Carbon

– TOC, Total Nitrogen –TN, both expressed in %) and stable isotope measurements ($\delta^{13}C$ and $\delta^{15}N$, expressed in ‰). These measurements were performed with a continuous flow Elementar® VarioPyro cube analyzer coupled to a Micromass® Isoprime IRMS available at the Alysés platform of the Institut de Recherche pour le Développement (Bondy, France) on a selection of 41 samples (respectively 29 samples for the RDB-01 core and 12 samples for the PA-02). Organic matter properties measured in both cores are provided in an open access Zenodo dataset (https://zenodo.org/record/6630479#.YqiFLuzP2Uk).

Mixing model

Temporal reconstruction of the sediment source contributions accumulated in the reservoirs and their evolution with time was achieved through the comparison of the organic matter properties (TOC, TN, $\delta^{13}C$ and $\delta^{15}N$) measured in the sediment cores with those analyzed in potential soil sources (soil samples from cropland and natural grassland, under the form of composite samples - 10 subsamples collected in a radius of 100 meters – from the upper 0-2 cm surface soil layer) from previous studies conducted in the Campos biome in Southernmost Brazil [46]. Soil composite samples were taken in representative areas of each land use, i.e. cropland including rice, soybean and mixed farming fields (n=36), and native grassland (n=31) which is generally used to extensively feed livestock. Soil from the upper 0-2 cm layer was collected, as this layer is the most likely to be eroded and transported to the river network. For each composite source sample, around 10 sub-samples were collected within a radius of approximately 50 meters, mixed in a bucket and approximately 500 grams of material were stored. Care was taken to avoid sites that have accumulated sediment originating from other sources, to prevent the collection of transient material. The source sampling sites were selected in order to cover all the soil types and the variability in slope positions of a 5,943-km² basin. More details and a map showing the soil sampling distribution can be found in Ramon (2021) [46].

TOC and TN in Brazilian grassland [46] varied between 46.2 ±16.1 g kg^{-1} and 4.5 ±1.5 g kg^{-1}, respectively. In cropland, TOC and TN concentrations amounted to 32.7 ± 9.1 g kg^{-1} and 3.3 ± 0.8 g kg^{-1}. These results are consistent with those of Sämuel et al. [47] who conducted similar measurements at 28 monitoring sites across Uruguay. They found that in grassland, TOC reached 29 ±19 g kg^{-1} (n = 115), while TN amounted to 2.2 ±1.3 g kg^{-1} (n = 115). Under cropland, TOC reached 26 ±7 g kg^{-1} (n = 15), and TN amounted to 2.2 ±0.6 g kg^{-1} (n = 15). These concentrations were slightly lower than those obtained by Ramon (2021) [46], which is very likely explained by the fact that different soil depths were targeted by both studies (i.e. 0–10 cm layer for Sämuel et al. [47], vs. 0–2cm for Ramon (2021) [46]) and the uppermost layer is known to be the most enriched in organic matter. Under native forest, TOC was 42 ±36 g kg^{-1} (n = 15), and TN amounted to 3.0 ±1.9 g kg^{-1} (n = 15). Finally, in forest plantations, TOC was 25 ±15 g kg^{-1} (n = 93), and TN was 1.8 ±1.0 g kg^{-1} (n = 93). The source database used in this study can be found in Ramon (2021) [46].

Tracer selection and source apportionments were performed following three steps: i) a range test; ii) a Mann Whitney *U* test (MW *U* test); and iii) a linear discriminant function analysis (LDA). For passing the range test, mean parameters values for sediment must fall within the range between the maximum and minimum values observed in the sources. The MW *U* test was then performed to test the null hypothesis ($p < 0.05$) that the sources belong to the same population. A forward stepwise LDA ($p < 0.1$) was applied to the variables that provided significant discrimination between the sources to reduce the number of variables to a minimum that maximizes source discrimination [48]. The statistical analyses were performed with R software [49].

A mass balance un-mixing model was applied to calculate the source contributions to individual sediment layers by minimizing the sum of squared residuals (SSR).

$$SSR = \sum_{i=1}^{n} \left(\left(C_i - \left(\sum_{s=1}^{m} P_s S_{si} \right) \right) / C_i \right)^2 \tag{1}$$

where n is the number of variables/elements used for modelling, C_i is the value of the parameter i in the target sediment (i.e. succession of sediment layers in both reservoirs), m is the number of sources, P_s is the optimized relative contribution of source s obtained by the SSR minimizing function, and S_{si} is the concentration of element i in the source s.

To ensure that the contributions did not result in negative values and that the sum of the contributions from all sources was equal to 1, restrictions were applied in the optimization process. To evaluate the uncertainty, the un-mixing model was solved by a Monte Carlo simulation with 2500 iterations, following the methods described in Batista et al. [50].

Data availability Statement

Dataset are available in ZENODO repository at https://zenodo.org/record/6630369 and https://zenodo.org/record/6630479

Acknowledgments

Collaboration between France and Uruguay is supported by an applied research project from the Fondo Maria Viñas (FMV_1_2019_1_156244, authors who received this funding M.T, G.C, M.C, J.G, P.C and O.E funded by the National Agency of Research and Innovation (ANII, Uruguay). This work gave inspiration to the AVATAR project (ANR-22-CE93-0001).

Author Contributions Statement: M.T, G.C, M.C, J.G, P.C have collected the sediment cores. AC. S, M.A have carried out CT-Scan measurements. A.F has performed gamma and organic matter analyses as well as the XRF core scanner measurements. R.R and T.T have developed the sediment tracing approach. A.F, PA. C and O.E drafted the manuscript. All co-authors have participated to the redaction and review.

Competing Interest Statement: The authors declare no competing interest.

Figure caption

Fig 1. Location of the study sites within the Rio Negro Basin, Uruguay – Land use pattern in the Rincón del Bonete and Palmar catchments base on the open access Land Use Atlas of Uruguay (FAO)

Fig 2. Evolution of the main land uses between 2000 and 2015 for the Palmar (A) and Rincón del Bonete (B) catchments based on the Land Use Atlas of Uruguay (FAO) (left panel). Evolution of the soybean and natural grassland surface areas (C) as estimated from the FAO database at the Uruguayan scale (right panel).

Fig 3. Age-depth models of the Rincón del Bonete (RDB-01) and Palmar (PA-02) sediment cores based on the CF:CS model computed from 10 and 7 gamma spectrometry measurements (respectively A and B). Vertical error bars correspond to the thickness of the analyzed layer. The horizontal error bars represent the analytical error.

Fig 4. Evolution of the Mass Accumulation Rate (MAR), the terrigenous fraction proxy (Fe) and the contribution of the natural grassland source to sediment accumulated in the Rincon del Bonete

(RDB) and Palmar (PA) reservoirs. The grey zones show the periods of change in accumulation of sediment and terrigenous material corresponding to (1) the planting of exotic tree species in RDB catchment (mostly eucalyptus), (2) the economic crisis in Uruguay (2000-2002) associated with a drop of the cultivated areas, (3) the planting of a mix of exotic trees associated with the expansion of agriculture in RDB catchment vs. the expansion of agriculture alone in PA catchment.

References

1. Tilman, D., Balzer, C., Hill, J. & Befort, B. L. Global food demand and the sustainable intensification of agriculture. *Proc. Natl. Acad. Sci. U. S. A.* **108**, 20260–20264 (2011).

2. Jaurena, M. *et al.* Native Grasslands at the Core: A New Paradigm of Intensification for the Campos of Southern South America to Increase Economic and Environmental Sustainability. *Front. Sustain. Food Syst.* **5**, (2021).

3. Zalles, V. *et al.* Rapid expansion of human impact on natural land in South America since 1985. *Sci. Adv.* **7**, (2021).

4. Song, X.-P. *et al.* Massive soybean expansion in South America since 2000 and implications for conservation. *Nat. Sustain.* **4**, 784–792 (2021).

5. MGAP- DIEA. *Encuesta agrícola "Primavera 2007" Serie encuestas Nº 257*. (2008).

6. Chiappe, M., Carambula, M. & Fernandez, E. *El campo uruguayo: una mirada desde la sociologia rural.* (2008).

7. Peake, L. R. & Robb, C. The global standard bearers of soil governance. *Soil Secur.* **6**, 100055 (2022).

8. García-Préchac, F. *et al.* Long-Term Effects of Different Agricultural Soil Use and Management Systems on Soil Degradation in Uruguay. in *Global Degradation of Soil and Water Resources* 77–92 (Springer Nature Singapore, 2022). doi:10.1007/978-981-16-7916-2_7

9. Alonso, J., Audicio, P., Martinez, L., Scavone, M. & Rezzano, E. Comparison of

measured 137Cs data and USLE/ RUSLE simulated long-term erosion rates. *Agrociencia Uruguay* **16**, (2012).

10. Didoné, E. J., Minella, J. P. G. & Evrard, O. Measuring and modelling soil erosion and sediment yields in a large cultivated catchment under no-till of Southern Brazil. *Soil Tillage Res.* **174**, 24–33 (2017).

11. Minella, J. P. G. *et al.* Long-term sediment yield from a small catchment in southern Brazil affected by land use and soil management changes. *Hydrol. Process.* **32**, 200–211 (2018).

12. Tassano, M. *et al.* Evaluation of soil erosion and sediment sources in two contrasting sub-basins, using fingerprinting and 137Cs techniques in Uruguay. Preliminary results. *EGU21* (2021). doi:10.5194/EGUSPHERE-EGU21-6466

13. Tiecher, T. *et al.* Fingerprinting sediment sources in a large agricultural catchment under no-tillage in Southern Brazil (Conceição River). *L. Degrad. Dev.* **29**, 939–951 (2018).

14. Brazeiro, A., Achkar, M., Toranza, C. & Bartesaghi, L. Agricultural expansion in Uruguayan grasslands and priority areas for vertebrate and woody plant conservation. *Ecol. Soc. Publ. online Feb 24, 2020 | doi10.5751/ES-11360-250115* **25**, (2020).

15. Laborde, A. *et al.* Children's Health in Latin America: The Influence of Environmental Exposures. *Environ. Health Perspect.* **123**, 201 (2015).

16. Vihervaara, P., Marjokorpi, A., Kumpula, T., Walls, M. & Kamppinen, M. Ecosystem services of fast-growing tree plantations: A case study on integrating social valuations with land-use changes in Uruguay. *For. Policy Econ.* **14**, 58–68 (2012).

17. Reichert, J. M., de Deus Junior, J. C., Borges Junior, N. & Cavalcante, R. B. L. Experimental catchments in the Pampa biome: Database on hydrology in grasslands and eucalyptus plantations in subtropical Brazil. *Hydrol. Process.* **35**, (2021).

18. Ramon, R. *et al.* Combining spectroscopy and magnetism with geochemical tracers to improve the discrimination of sediment sources in a homogeneous subtropical catchment. *CATENA* **3535**, 104800 (2020).

19. Foucher, A. *et al.* Deciphering human and climatic controls on soil erosion in intensively

cultivated landscapes after 1950 (Loire Valley, France). *Anthropocene* **34**, 100287 (2021).

20. Bajard, M. *et al.* Erosion record in Lake La Thuile sediments (Prealps, France): Evidence of montane landscape dynamics throughout the Holocene. *The Holocene* **26**, 350–364 (2015).

21. Baud, A., Jenny, J.-P., Francus, P. & Gregory-Eaves, I. Global acceleration of lake sediment accumulation rates associated with recent human population growth and land-use changes. *J. Paleolimnol. 2021 664* **66**, 453–467 (2021).

22. Sabatier, P. *et al.* Evidence of Chlordecone Resurrection by Glyphosate in French West Indies. *Environ. Sci. Technol.* **55**, 2296–2306 (2021).

23. Foucher, A. *et al.* Regional trends in eutrophication across the Loire river basin during the 20th century based on multi-proxy paleolimnological reconstructions. *Agric. Ecosyst. Environ.* **301**, (2020).

24. Foucher, A., Chaboche, P., Sabatier, P. & Evrard, O. A worldwide meta-analysis (1977 – 2020) of sediment core dating using fallout radionuclides including 137Cs and 210Pbxs. *Earth Syst. Sci. Data* **13**, 4951–4966 (2021).

25. Chaboche, P. *et al.* 240Pu/239Pu signatures allow refining the chronology of radionuclide fallout in South America. *Sci. Total Environ.* **843**, 156943 (2022).

26. Terra, J. . & García-Prèchac, F. *Efecto de la intensidad de uso y laboreo sobre el recurso suelo y su calidad In Terra*. (2001).

27. Polla, M. C. agroforestería en Uruguay. *Dirección de Recursos Forestales, FAO* (1997). Available at: https://agris.fao.org/agris-search/search.do?recordID=US201300062307. (Accessed: 14th April 2022)

28. Geary, T. F. Afforestation in Uruguay: Study of a Changing Landscape. *J. For.* **99**, 35–39 (2001).

29. DIEA. *Encuesta agrícola " invierno 2020*. (2020).

30. Oliveira, A. H. *et al.* Water erosion in soils under eucalyptus forest as affected by development stages and management systems. *Ciência e Agrotecnologia* **37**, 159–169

(2013).

31. Valente, M. L. *et al.* Afforestation of degraded grasslands reduces sediment transport and may contribute to streamflow regulation in small catchments in the short-run. *CATENA* **204**, 105371 (2021).

32. Redo, D. J., Aide, T. M., Clarck, M. L. & Andrade-Nunez, M. J. Impacts of internal and external policies on land change in Uruguay, 2001–2009. *Environ. Conserv.* **39**, 122–131 (2012).

33. Zurbriggen, C. *et al.* Experimentation in the design of public policies: The uruguayan soils conservation plans. *Iberoam. - Nord. J. Lat. Am. Caribb. Stud.* **49**, 52–62 (2020).

34. Mendez-Millan, M. *et al.* Compound-specific 13C and 14C measurements improve the understanding of soil organic matter dynamics. *Biogeochemistry* **118**, 205–223 (2014).

35. Del Galdo, I., Six, J., Peressotti, A. & Francesca Cotrufo, M. Assessing the impact of land-use change on soil C sequestration in agricultural soils by means of organic matter fractionation and stable C isotopes. *Glob. Chang. Biol.* **9**, 1204–1213 (2003).

36. Foucher, A. *et al.* Persistence of environmental DNA in cultivated soils: implication of this memory effect for reconstructing the dynamics of land use and cover changes. *Sci. Rep.* (2020). doi:10.1038/s41598-020-67452-1

37. Alexandratos, N. & Bruinsma, J. *World Agriculture Towards 2030/2050: The 2012 Revision*. (2012).

38. Nin-Pratt, A., Freiría, H. & Muñoz, G. Productivity and Efficiency in Grassland-based Livestock Production in Latin America: The Cases of Uruguay and Paraguay. (2019). doi:10.18235/0001924

39. Mthimkhulu, S., Podwojewski, P., Hughes, J., Titshall, L. & Van Antwerpen, R. The effect of 72 years of sugarcane residues and fertilizer management on soil physico-chemical properties. *Agric. Ecosyst. Environ.* **225**, 54–61 (2016).

40. Chalar, G., Gerhard, M., González-Piana, M. & Fabián, D. *Hidroquímica y eutrofización en tres embalses subtropicales en cadena*. *Procesos Geoquímicos Superficiales en Iberoamérica* (2014).

41. González-Piana, M. *et al.* Effects of Wind Mixing in a Stratified Water Column on Toxic Cyanobacteria and Microcystin-LR Distribution in a Subtropical Reservoir. *Bull. Environ. Contam. Toxicol. 2018 1015* **101**, 611–616 (2018).

42. Didoné, E. J. *et al.* Mobilization and transport of pesticides with runoff and suspended sediment during flooding events in an agricultural catchment of Southern Brazil. *Environ. Sci. Pollut. Res.* **28**, 39370–39386 (2021).

43. Appleby, P. G. & Oldfield, F. The calculation of lead-210 dates assuming a constant rate of supply of unsupported210Pb to the sediment. *Catena* **5**, 1–8 (1978).

44. Bruel, R. & Sabatier, P. serac: A R package for ShortlivEd RAdionuclide chronology of recent sediment cores. *J. Environ. Radioact.* **225**, (2020).

45. Croudace, I. W. & Rothwell, R. G. *Micro-XRF Studies of Sediment Cores*. *Developments in Paleoenvironmental Research* **17**, (Springer Netherlands, 2015).

46. Ramon, R. Quantifying sediment source contributions in contrasted agricultural catchments (Uruguay River, Southern Brazil). (Paris-Saclay, 2021).

47. Säumel, I., Ramírez, L. R., Tietjen, S., Barra, M. & Zagal, E. Back to the future-Conservative grassland management for Anthropocene soils in the changed landscapes of Uruguay ? *Egusph. [preprint]* (2022). doi:10.5194/egusphere-2022-335

48. Collins, A. L., Zhang, Y. & Walling, D. E. Apportioning sediment sources in a grassland dominated agricultural catchment in the UK using a new tracing framework. in *Sediment Dynamics for a Changing Future* **337**, 68–75 (2010).

49. R Development Core Team. R: a language and environment for statistical computing. (2020).

50. Batista, P. V. G. *et al.* Using pedological knowledge to improve sediment source apportionment in tropical environments. *J. Soils Sediments* **19**, 3274–3289 (2019).

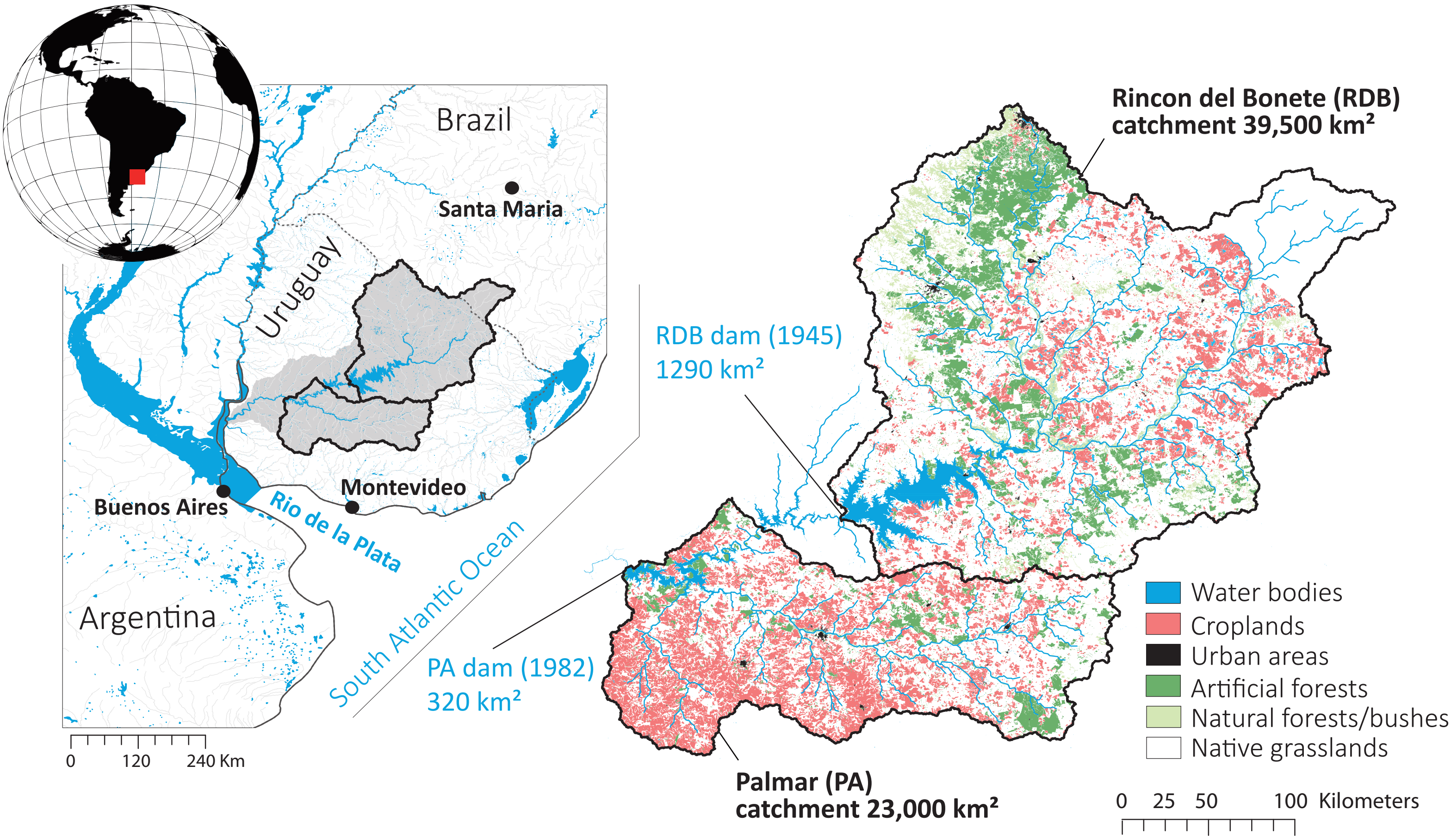

Brazil
Santa Maria
Uruguay
Argentina
Buenos Aires
Montevideo
Rio de la Plata
South Atlantic Ocean
0
120
240 Km
Rincon del Bonete (RDB)
catchment 39,500 km²
RDB dam (1945)
1290 km²
PA dam (1982)
320 km²
Palmar (PA)
catchment 23,000 km²
Water bodies
Croplands
Urban areas
Artificial forests
Natural forests/bushes
Native grasslands
0 25 50 100 Kilometers

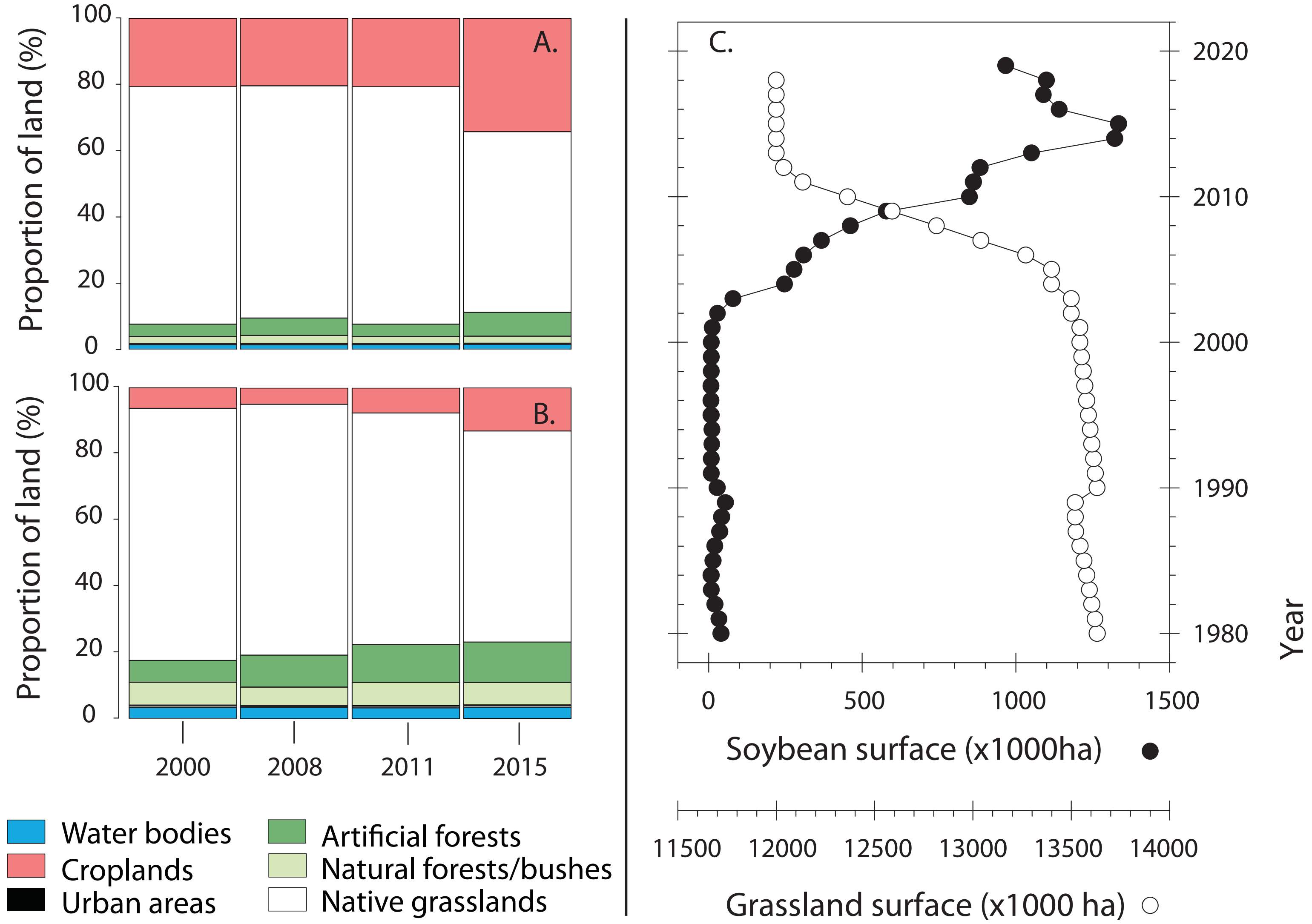

A.
B.
C.
Proportion of land (%)
Proportion of land (%)
0
20
40
60
80
100
2000
2008
2011
2015
Water bodies
Croplands
Urban areas
Artificial forests
Natural forests/bushes
Native grasslands
Year
1980
1990
2000
2010
2020
0
500
1000
1500
Soybean surface (x1000ha)
11500
12000
12500
13000
13500
14000
Grassland surface (x1000 ha)

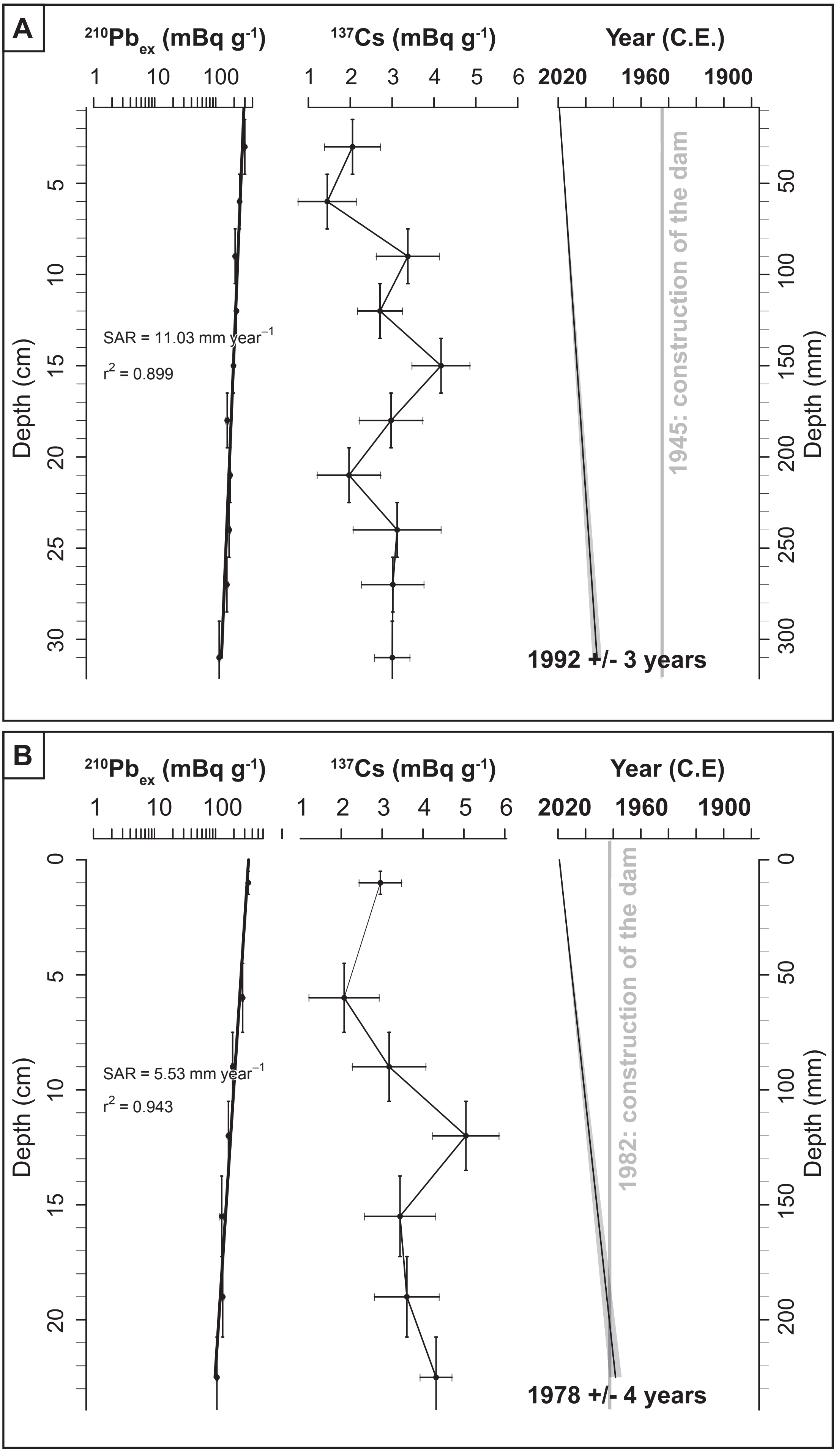
A
$^{210}Pb_{ex}$ (mBq g^{-1})
^{137}Cs (mBq g^{-1})
Year (C.E.)
SAR = 11.03 mm year^{-1}
r^2 = 0.899
1945: construction of the dam
1992 +/- 3 years
Depth (cm)
Depth (mm)
B
$^{210}Pb_{ex}$ (mBq g^{-1})
^{137}Cs (mBq g^{-1})
Year (C.E)
SAR = 5.53 mm year^{-1}
r^2 = 0.943
1982: construction of the dam
1978 +/- 4 years
Depth (cm)
Depth (mm)

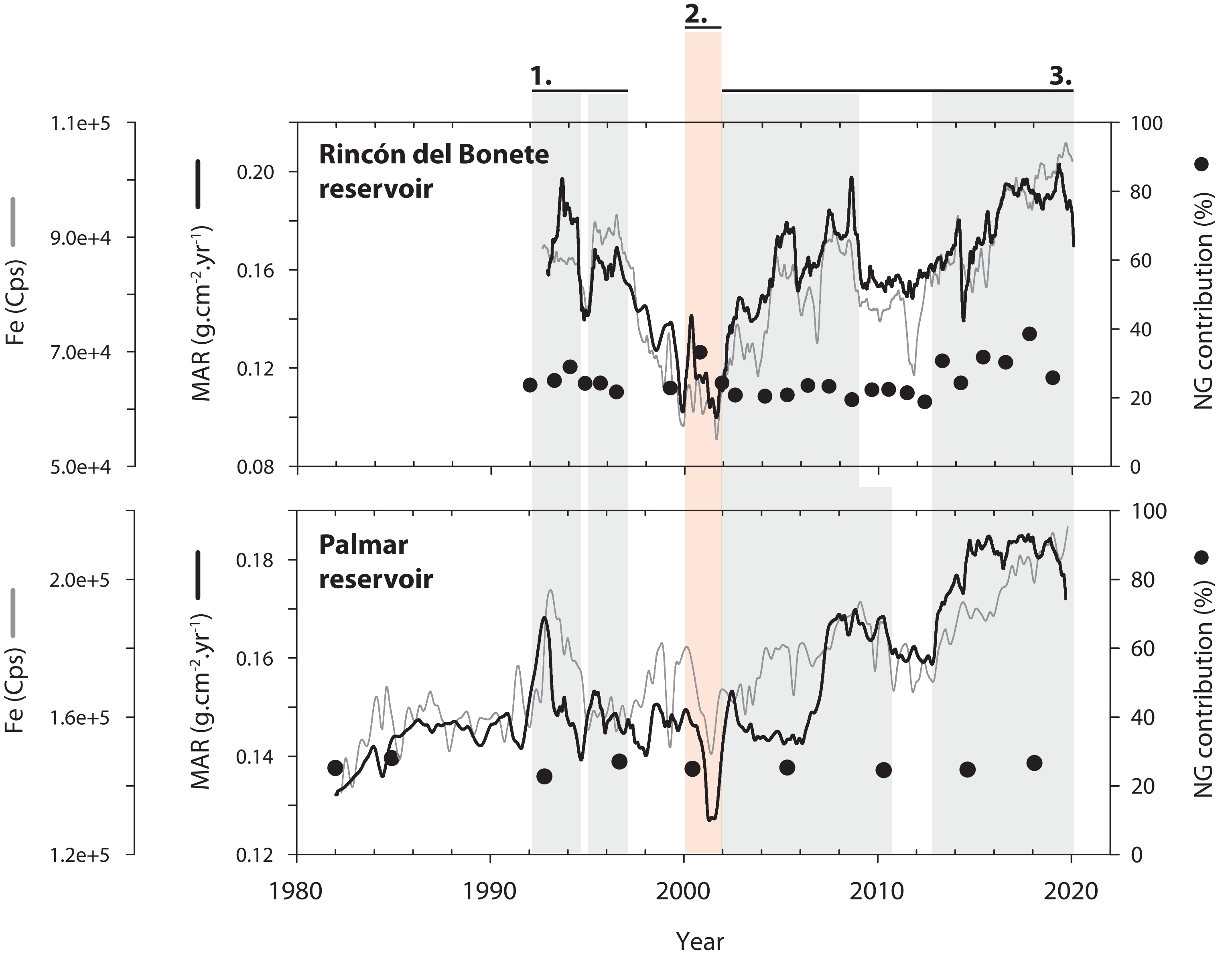
1.
2.
3.
Rincón del Bonete reservoir
Palmar reservoir
Fe (Cps)
MAR (g.cm-2.yr-1)
NG contribution (%)
1.1e+5
9.0e+4
7.0e+4
5.0e+4
0.20
0.16
0.12
0.08
100
80
60
40
20
0
2.0e+5
1.6e+5
1.2e+5
0.18
0.16
0.14
0.12
1980
1990
2000
2010
2020
Year